Earthquakes and Structures, *Vol. 11, No. 1 (2016) 45-61*
DOI: http://dx.doi.org/10.12989/eas.2016.11.1.045

A method for dynamic analysis of frame-hinged shear wall structures

Kanat Burak Bozdogan[*1] and Duygu Öztürk[2a]

[1]*Department of Civil Engineering, Canakkale Onsekiz Mart University, Canakkale, Turkey*
[2]*Department of Civil Engineering, Ege University, Izmir, Turkey*

(Received October 31, 2015, Revised May 23, 2016, Accepted June 10, 2016)

Abstract. Structures with soft story irregularity have been seriously damaged in earthquakes. Therefore, the analysis of dynamic behavior of structures with soft story irregularity is of great value and relevance.

In this study, a certain method will be used to discover the displacements and internal forces and to find out results about soft story irregularity. For this study, the multi-story frame-hinged shear wall system has been used as a model according to the continuous calculation system. The dynamic characteristics of the system have been obtained by analyzing the governing differential equation of the system. The dynamic characteristics have been calculated for a practical and quick analysis as indicated in tables. The suggested method is wholly based on manual calculation. A spectral analysis can be easily conducted with the help of Tables provided by this study.

A sample has been solved and compared to the finite elements method to study the suitability of the method suggested at the end of this study.

Keywords: dynamic analysis; continuous system; multistory structure; hinged shear wall; frame

1. Introduction

Many structures with soft story irregularity have been either seriously damaged, or fully collapsed in earthquakes that have taken place throughout history. Large displacements that occur on the soft story result in damage or total collapse of these types of structures. Therefore, it is important to accurately determine the dynamic behavior of these types of structures.

A series of studies concerning the soft story is presented in the literature. Two of them are summarized below.

Colunga (2010) conducted a study to determine the soft story irregularity on the first floor. For this purpose, the method presented by the author is investigated by comparing with the equation for determining the soft story irregularity in the Mexican Earthquake Code. Abidi *et al*. (2012) studied the soft story irregularity in shear wall structures.

The continuous system calculation method is a method used in static, dynamic, and stability analysis of multi-story structures and buildings. It is really useful and helpful in understanding the

*Corresponding author, Associate Professor, E-mail: kbbozdogan@yahoo.com.tr
[a]Ph.D., E-mail: duyguozturk@hotmail.com

 ISSN: 2092-7614 (Print), 2092-7622 (Online)

behavior of these kinds of structures and in analyzing the stages of preliminary sizing.

There have been many studies (Rosman 1964, Rosman 1974, Heidebrecht and Stafford 1974, Bilyap 1979, Rosman 1981, Baikov and Sigalov 1983, Balendra *et al*. 1984, Basu *et al*. 1984, Stafford Smith and Crowe 1986, Nollet and Stafford Smith 1993, Toutanji 1997, Wang 1997, Mancini and Savassi 1999, Miranda 1999, Quanfeng *et al*. 1999, Kuang and Ng 2000, Wang *et al*. 2000, Ng and Kuang 2000, Zalka 2000, Swaddiwudhipong *et al*. 2001, Hoenderkamp 2001, Zalka 2001, Hoenderkamp 2002, Miranda and Reyes 2002, Potzta and Kollar 2003, Savassi and Mancini 2004, Tarjan and Kollar 2004, Miranda and Taghavi 2005, Taghavi and Miranda 2005, Reinoso and Miranda 2005, Georgoussis 2006, Dym and Williams 2007, Rafezy *et al*. 2007, Kaviani *et al*. 2008, Laier 2008, Meftah and Tounsi 2008, Rafezy and Howson 2008, Savassi and Mancini 2009, Bozdogan 2009, Zalka 2009, Kuang and Ng 2009, Yang *et al*. 2010, Kazaz and Gulkan 2012, Jahanshahi and Rahgozar 2012, Wdowicki and Wdowicka 2012, Al-Aasam and Mandal 2013, Carpinteri *et al*. 2013, Zalka 2013, Malekinejad and Rahgozar 2013, Georgoussis 2014, Zalka 2014, Belhadj and Meftah 2015, Rodriguez and Miranda 2015, Tekeli *et al*. 2015) done in this field of academia that have used the continuous system calculation method. Pan *et al*. (2015) have modeled structures according to the continuous system calculation model to examine the impact of soft story irregularity. Their results have helped researchers discover a deeper understanding of the displacement and internal forces relations for three different static loading situations. They compared a five-story sample analyzed by using the method they suggested at the end of this study with the SAP2000 program. In consideration of the results, they found a difference between the method they suggested and the SAP2000 program by a maximum 12%.

In this study, the method suggested by Pan et al. for static analysis has been developed for dynamic analysis, and the results have been tabulated for easy and quick use. Therefore, the analysis can be quickly conducted with the help of the tables provided by this study. In the development of the equations and tables obtained during the study, the following have been accepted:

a) Material is linear elastic.

b) It has been accepted that the displacements are small. Because of this, the geometric non-linearity is disregarded.

c) It has been accepted that the material and geometric characteristics are uniform throughout the height of the structure.

d) Shear walls are modeled as bending beams and the shear displacements of the shear walls have been disregarded.

e) Shear wall is considered as hinged supported.

f) The frame element is modeled as shear beam and the axial displacement is taken into account by multiplying the equivalent shear stiffness by a correction coefficient.

g) Torsion impacts have been disregarded.

2. Mathematical model

The multi-story frame-hinged shear wall system can be shown as an equivalent of a bending-shear beam (Fig. 1). In Fig. 1, the rods with hinges on both ends represent the slabs on the floor levels and are continuously rigid within their own planes.

According to the model, the following governing differential equation is written for the free vibration analysis as indicated above

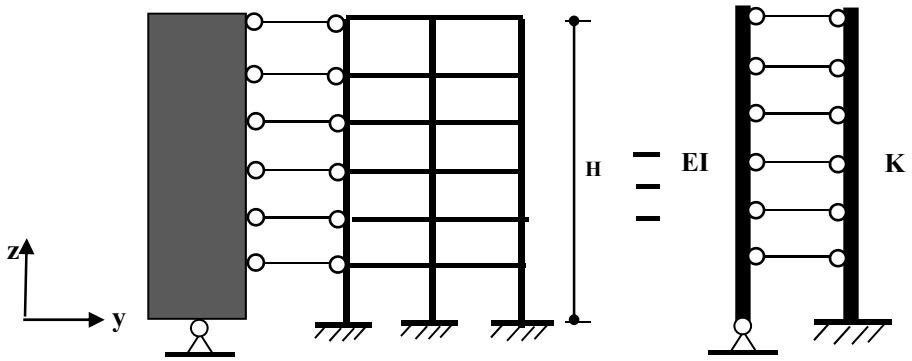

Fig. 1 Equivalent model of frame hinged shear wall structures

$$EI\frac{\partial^4 y}{\partial z^4} - K\frac{\partial^2 y}{\partial z^2} + \frac{m}{h}\frac{\partial^2 y}{\partial t^2} = 0 \tag{1}$$

where *m* represents the mass of the story, *h* symbolizes the height of the story, and *z* indicates the vertical axis throughout the height of the structure.

EI represents the total bending stiffness of the shear walls. It is calculated using the following equation. (Zalka 2000)

$$EI = \sum_{i=1}^{f} EI_i \tag{2}$$

where *f* represents the number of shear walls.

K indicates the equivalent shear stiffness. It is calculated using the following equation. (Baikov and Sigalov 1983)

$$K = \frac{12}{h*(\frac{1}{r}+\frac{1}{s})} \tag{3}$$

The representation of *r* is the contribution of beams to the shear stiffness and *s* indicates the contribution of columns to the shear stiffness. These are calculated using the following calculations

$$r = \sum_{i=1}^{p} \frac{EI_{bi}}{l_i} \tag{4}$$

$$s = \sum_{i=1}^{q} \frac{EI_{ci}}{h} \tag{5}$$

Respectively, *p* and q indicate the numbers of beams and columns on a floor. When Eq. (1) is separated into its variables based on position and time using Eq. (6), the ordinary differential equations will be achieved as displayed under Eqs. (7) and (8).

$$Y(z,t) = A(z) * B(t) \tag{6}$$

$$EI\frac{d^4A}{dz^4} - K\frac{d^2A}{dz^2} - \frac{\omega^2 m}{h}A = 0 \tag{7}$$

$$\frac{d^2B}{dt^2} + \omega^2 B = 0 \tag{8}$$

A illustrates the mode shape function and ω illustrates the angular frequency.

In the system displayed in Fig. 1, the displacement and the bending moment at the bottom of the structure and the bending moment with the shear force at the top is zero. The boundary conditions as specified can be shown using the Eqs. (9), (10), (11) and (12)

$$z = 0 \qquad \mathrm{A} = 0 \tag{9}$$

$$z = 0 \qquad \mathrm{EI}\frac{d^2A}{dz^2} = 0 \tag{10}$$

$$z = H \qquad \mathrm{EI}\frac{d^2A}{dz^2} = 0 \tag{11}$$

$$z = H \qquad \mathrm{EI}\frac{d^3A}{dz^3} - K\frac{dA}{dz} = 0 \tag{12}$$

If the transformation as indicated in Eq. (13) restores the Eq. (7) dimensionless, the following Eq. (14) will be achieved

$$\varepsilon = \frac{z}{H} \tag{13}$$

$$\frac{EI}{H^4}\frac{d^4A}{d\varepsilon^4} - \frac{K}{H^2}\frac{d^2A}{d\varepsilon^2} - \frac{\omega^2 m}{h}A = 0 \tag{14}$$

If rearrangements are made in to the Eq. (14), Eq.(15) will be achieved.

$$\frac{d^4A}{d\varepsilon^4} - \frac{KH^2}{EI}\frac{d^2A}{d\varepsilon^2} - \frac{\omega^2 mH^4}{hEI}A = 0 \tag{15}$$

If the definitions as given under Eqs. (16) and (17) are made to simplify the notation of the Eq. (15), Eq. (18) can be created

$$k = H\sqrt{\frac{K}{EI}} \tag{16}$$

$$\alpha = \frac{\omega^2 mH^4}{hEI} \tag{17}$$

$$\frac{d^4A}{d\varepsilon^4} - k^2\frac{d^2A}{d\varepsilon^2} - \alpha A = 0 \tag{18}$$

If the boundary conditions as given in Eqs. (9), (10), (11) and (12) are also made dimensionless, then the boundary conditions can be expressed as below

$$\varepsilon = 0 \qquad \mathrm{A} = 0 \tag{19}$$

$$\varepsilon = 0 \qquad \frac{1}{\mathrm{H}^2}\frac{d^2A}{d\varepsilon^2} = 0 \tag{20}$$

$$\varepsilon = 1 \qquad \frac{1}{\mathrm{H}^2}\frac{d^2A}{d\varepsilon^2} = 0 \tag{21}$$

$$\varepsilon = 1 \qquad \frac{d^3A}{d\varepsilon^3} - k^2\frac{dA}{d\varepsilon} = 0 \tag{22}$$

The solution for the Eq. (18) is given below.

$$A(\varepsilon) = c_1\cos(\beta_1\varepsilon) + c_2\sin(\beta_1\varepsilon) + c_3\cosh(\beta_2\varepsilon) + c_4\sinh(\beta_2\varepsilon) = 0 \tag{23}$$

$$\beta_1 = \sqrt{\sqrt{(\frac{k^4}{4} + \alpha)} - \frac{k^2}{2}} \tag{24}$$

$$\beta_2 = \sqrt{\sqrt{(\frac{k^4}{4} + \alpha)} + \frac{k^2}{2}} \tag{25}$$

If the boundary conditions as given in Eqs. (19) to (22) are applied to the integration constants c_1, c_2, c_3, c_4 as contained in Eq. (23), the matrix Eq. (26) will be achieved

$$\begin{bmatrix} -\beta_1^2\sin(\beta_1) & \beta_2^2\sinh(\beta_2) \\ (-\beta_1^3 - k^2\beta_1)\cos(\beta_1) & (\beta_2^3 - k^2\beta_2)\cosh(\beta_2) \end{bmatrix}\begin{Bmatrix} c_2 \\ c_4 \end{Bmatrix} = \begin{Bmatrix} 0 \\ 0 \end{Bmatrix} \tag{26}$$

To have a non-zero solution of the Eq. (26), the determinant of the matrix must be zero

$$(k^2\beta_1^2\beta_2 - \beta_1^2\beta_2^3)\cosh(\beta_2)\sin(\beta_1) + (\beta_1^3\beta_2^2 + k^2\beta_1\beta_2^2)\cos(\beta_1)\sinh(\beta_2) \tag{27}$$

After α values which offers the Eq. (27) are found, ω values are found with the help of the Eq. (17).

The mode shape is calculated using the Eq. (28)

$$A(\varepsilon) = c_2[\sin(\beta_1\varepsilon) + \frac{\beta_1^2\sin(\beta_1)}{\beta_2^2\sinh(\beta_2)}\sinh(\beta_2\varepsilon)] \tag{28}$$

As the Eq. (28) represents the mode shape, the c_2 value can be considered 1, and the mode shape can be defined using the following equation

$$A(\varepsilon) = [\sin(\beta_1 \varepsilon) + \frac{{\beta_1}^2 \sin(\beta_1)}{{\beta_2}^2 \sinh(\beta_2)} \sinh(\beta_2 \varepsilon)] \tag{29}$$

Using the frequency equation, the *i.* period value is calculated using the following equation

$$T_i = S_i H^2 \sqrt{\frac{m}{hEI}} \tag{30}$$

The *S* values in the equation are calculated for the first three modes, and given in Table 1.

For the modal participation factor, the following equation can be written down as it is in many other similar studies and literature

$$\Gamma_i = \frac{\int_0^1 \frac{m}{h} A_i(\varepsilon) d\varepsilon}{\int_0^1 \frac{m}{h} {A_i}^2(\varepsilon) d\varepsilon} \tag{31}$$

If the mode shape function contained in Eq. (29) is put into its place in Eq. (31), then the participation factors for the first three modes shall be calculated as given in Table 2.

Table 1 S_i values for the first three modes

k	S_1	S_2	S_3	k	S_1	S_2	S_3	k	S_1	S_2	S_3
0.0	-	0.4080	0.1260	8.0	0.4929	0.1484	0.0758	16	0.2490	0.0803	0.0455
1.0	3.6590	0.3861	0.1240	9.0	0.4393	0.1345	0.0703	17	0.2344	0.0759	0.0432
2.0	1.8640	0.3381	0.1192	10.0	0.3961	0.1229	0.0654	18	0.2215	0.0719	0.0411
3.0	1.2653	0.2880	0.1122	11.0	0.3606	0.1131	0.0611	19	0.2099	0.0683	0.0392
4.0	0.9621	0.2458	0.1044	12.0	0.3310	0.1046	0.0573	20	0.1994	0.0651	0.0375
5.0	0.7771	0.2124	0.0964	13.0	0.3058	0.0973	0.0538	30	0.1332	0.0439	0.0259
6.0	0.6519	0.1862	0.0888	14.0	0.2842	0.0909	0.0507				
7.0	0.5614	0.1653	0.0820	15.0	0.2654	0.0853	0.0480				

Table 2 Γ_i are the values for the first three modes

				Γ_i							
k	Γ_1	Γ_2	Γ_3	k	Γ_1	Γ_2	Γ_3	k	Γ_1	Γ_2	Γ_3
0.0		0.5240	0.2826	8.0	1.2625	0.4112	0.2498	16	1.2718	0.4209	0.2509
1.0	1.0458	0.5037	0.2809	9.0	1.2655	0.4131	0.2491	17	1.2720	0.4214	0.2513
2.0	1.1072.	0.4644	0.2762	10.0	1.2675	0.4148	0.2488	18	1.2722	0.4218	0.2516
3.0	1.1746	0.4336	0.2700	11.0	1.2688	0.4164	0.2489	19	1.2723	0.4221	0.2519
4.0	1.2151	0.4168	0.2636	12.0	1.2698	0.4177	0.2492	20	1.2725	0.4224	0.2522
5.0	1.2377	0.4101	0.2581	13.0	1.2705	0.4188	0.2496	30	1.273	0.4238	0.2537
6.0	1.2504	0.4086	0.2541	14.0	1.2710	0.4196	0.2501				
7.0	1.2579	0.4095	0.2514	15.0	1.2714	0.4203	0.2505				

The effective modal mass ratios for the first three modes are calculated using the Eq. (32), and given in Table 3

$$eko_i = \frac{[\int_0^1 \frac{\mathrm{m}}{\mathrm{h}} \mathrm{A_i}(\varepsilon\varepsilon)\mathrm{d}\varepsilon^2}{\int_0^1 \frac{m}{h} A_i^{\,2}(\varepsilon)d\varepsilon} * \frac{h}{m} \tag{32}$$

The effective height value is calculated using the Eq. (33), and given in Table 4 for the first three modes

$$H^*_i = \frac{\int_0^1 \varepsilon A_i(\varepsilon)d\varepsilon}{\int_0^1 A_i(\varepsilon)d\varepsilon} \tag{33}$$

Using the spectrum of an earthquake record, the displacement function can be calculated using

Table 3 eko_i are values for the first three modes

	eko_i										
k	eko_1	eko_2	eko_3	k	eko_1	eko_2	eko_3	k	eko_1	eko_2	eko_3
0.0		0.1372	0.0399	8.0	0.81	0.09	0.033	16	0.81	0.09	0.032
1.0	0.76	0.13	0.040	9.0	0.81	0.09	0.033	17	0.81	0.09	0.032
2.0	0.77	0.12	0.039	10.0	0.81	0.09	0.033	18	0.81	0.09	0.032
3.0	0.79	0.10	0.038	11.0	0.81	0.09	0.033	19	0.81	0.090	0.032
4.0	0.80	0.10	0.036	12.0	0.81	0.09	0.032	20	0.81	0.09	0.032
5.0	0.80	0.09	0.035	13.0	0.81	0.09	0.032	30	0.81	0.09	0.032
6.0	0.80	0.09	0.034	14.0	0.81	0.09	0.032				
7.0	0.81	0.09	0.034	15.0	0.81	0.09	0.032				

Table 4 Effective height is for the first three modes

	H^*_I										
k	H^*_1	H^*_2	H^*_3	k	H^*_1	H^*_2	H^*_3	k	H^*_1	H^*_2	H^*_3
0.0		0.0032	0.0099	8.0	0.6386	0.2040	0.0967	16	0.6370	0.2151	0.1180
1.0	0.6631	0.0208	0.0038	9.0	0.6381	0.2070	0.1041	17	0.6369	0.2122	0.1225
2.0	0.6559	0.0686	0.0129	10.0	0.6378	0.2083	0.1120	18	0.6369	0.2135	0.1267
3.0	0.6495	0.1157	0.0316	11.0	0.6375	0.2075	0.1143	19	0.6368	0.2137	0.1290
4.0	0.6450	0.1509	0.0444	12.0	0.6373	0.2110	0.1129	20	0.6368	0.2090	0.1243
5.0	0.6423	0.1749	0.0625	13.0	0.6372	0.2119	0.1210	30	0.6367	0.2173	0.1158
6.0	0.6406	0.1888	0.0799	14.0	0.6370	0.2134	0.1257				
7.0	0.6394	0.1981	0.0863	15.0	0.6369	0.2130	0.1185				

the following equation

$$d_i(\varepsilon) = \Gamma_i * A_i(\varepsilon) * S_{di} \tag{34}$$

where S_{di} is the displacement spectrum ordinate as calculated for the i.th mode.

The maximum displacement value will take place at the top. It will be for ε=1

$$d_{\max i} = \Gamma_i * A_i(1) * S_{di} = \nu_i * S_{di} \tag{35}$$

The *v* values are calculated for the first three modes and provided in Table 5.

For the drift ratio, the Eq. (36) will be written like this below

$$IDR_i = \frac{\Gamma_i A'(\varepsilon) * S_{di}}{H} \tag{36}$$

The displacement function derivative will be calculated as provided below

$$A'(\varepsilon) = \frac{dA(\varepsilon)}{d\varepsilon} = [\beta_1 \cos(\beta_1 \varepsilon) + \frac{\beta_1^{\,2} \sin(\beta_1)}{\beta_2 \sinh(\beta_2)} \cosh(\beta_2 \varepsilon)] \tag{37}$$

To locate the maximum drift ratio, the derivative of the Eq. (37) has been calculated and evanished. It has been determined that the maximum drift ratio for the first three modes takes place at the bottom of the structure.

In such cases, the maximum drift ratio will be calculated using the Eq. (38)

$$\max(IDR_i) = \frac{\Gamma_i A'(0) * S_{di}}{H} = \frac{\eta_i * S_{di}}{H} \tag{38}$$

The η coefficient is calculated and provided for in Table 6 for the first three modes.

To determine the base shear force, the following Eq. can be used.

$$V_{Bi} = M * eko_i * S_{ai} \tag{39}$$

M indicates the total mass of the structure and S_{ai} indicates the ordinate value corresponding to the period in i. mode in the acceleration spectrum for the earthquake record. Eko_i indicates the

Table 5 ν_i coefficient is for the first three modes

	ν_i										
k	ν_1	ν_2	ν_3	k	ν_1	ν_2	ν_3	k	ν_1	ν_2	ν_3
0.0		0.74	-0.40	8.0	-1.31	0.51	-0.35	16	-1.28	0.45	-0.30
1.0	-1.48	0.72	-0.40	9.0	-1.30	0.50	-0.34	17	-1.28	0.45	-0.29
2.0	-1.44	0.68	-0.40	10.0	-1.30	0.49	-0.33	18	-1.28	0.45	-0.29
3.0	-1.40	0.63	-0.39	11.0	-1.29	0.48	-0.32	19	-1.28	0.45	-0.29
4.0	-1.37	0.60	-0.39	12.0	-1.29	0.47	-0.31	20	-1.28	0.44	-0.29
5.0	-1.35	0.57	-0.38	13.0	-1.29	0.46	-0.31	30	-1.28	0.43	-0.27
6.0	-.1.33	0.54	-0.38	14.0	-1.29	0.46	-0.31				
7.0	-1.32	0.52	-0.36	15.0	-1.29	0.46	-0.30				

Table 6 η_j coefficient is for the first three modes

	η_j										
k	η_1	η_2	η_3	k	η_1	η_2	η_3	k	η_1	η_2	η_3
0.0	-	2.000	2.000	8.0	1.974	1.887	1.884	16	1.997	1.974	1.950
1.0	1.5611	1.951	1.992	9.0	1.982	1.907	1.891	17	1.997	1.978	1.956
2.0	1.6859	1.868	1.970	10.0	1.986	1.924	1.899	18	1.997	1.981	1.960
3.0	1.797	1.813	1.942	11.0	1.989	1.938	1.909	19	1.998	1.983	1.965
4.0	1.872	1.800	1.915	12.0	1.992	1.950	1.918	20	1.998	1.985	1.969
5.0	1.918	1.813	1.895	13.0	1.994	1.957	1.927	30	2.000	1.996	1.988
6.0	1.946	1.837	1.884	14.0	1.995	1.964	1.936				
7.0	1.964	1.863	1.881	15.0	1.996	1.969	1.943				

Table 7 χ coefficient is for the first three modes

	χ_i										
k	χ_1	χ_2	χ_3	k	χ_1	χ_2	χ_3	k	χ_1	χ_2	χ_3
0.0		0.00044	0.0004	8.0	0.517	0.018	0.0032	16	0.516	0.019	0.0038
1.0	0.504	0.0027	0.00002	9.0	0.517	0.019	0.0034	17	0.516	0.019	0.0040
2.0	0.505	0.0082	0.0005	10.0	0.517	0.019	0.0037	18	0.516	0.019	0.041
3.0	0.513	0.012	0.0012	11.0	0.516	0.019	0.0038	19	0.516	0.019	0.0041
4.0	0.516	0.015	0.0016	12.0	0.516	0.019	0.0036	20	0.516	0.019	0.0040
5.0	0.514	0.016	0.0022	13.0	0.516	0.019	0.0039	30	0.516	0.020	0.0037
6.0	0.512	0.017	0.0027	14.0	0.516	0.019	0.0040				
7.0	0.518	0.018	0.0029	15.0	0.516	0.019	0.0038				

effective mass ratio in the i. mode. It will be taken from Table 3 for the first three modes.

The overturning moment that takes place at the base can be calculated using the following equation

$$M_{ot_i} = M * eko_i * H^* * S_{ai} = \chi_i * M * S_{ai} \tag{40}$$

The χ coefficients are given in Table 7 for the first three modes.

The bending moment equation can be calculated using the Eq. (41)

$$M_{wi}(\varepsilon) = \Gamma_i EI \frac{d^2 A(\varepsilon)}{d\varepsilon^2} = \frac{EI}{H^2} \Gamma_i [-\beta_1^2 \sin(\beta_1 \varepsilon) + \frac{\beta_1^2 \sin(\beta_1)}{\sinh(\beta_2)} \sinh(\beta_2 \varepsilon)] * S_d \tag{41}$$

To locate where the bending moment can be used to its maximum capacity throughout the structure height, the derivative of the Eq. (40) is calculated and evanished. The ε values are calculated and provided in Table 8 for the first three modes.

Maximum bending moment value will be calculated using the Eq. (42)

$$\max(M_{wi}) = \frac{EI}{H^2} \kappa S_d \tag{42}$$

Table 8 ε coefficient is for the first three modes

					ε_i						
k	ε_1	ε_2	ε_3	k	ε_1	ε_2	ε_3	k	ε_1	ε_2	ε_3
0.0		0.4191	0.2218	8.0	0.7013	0.3432	0.2083	16	0.7864	0.3347	0.2023
1.0	0.5813	0.4134	0.2214	9.0	0.7158	0.3407	0.2069	17	0.7934	0.3347	0.2019
2.0	0.5925	0.3992	0.2201	10.0	0.7289	0.3390	0.2057	18	0.7999	0.3344	0.2015
3.0	0.6092	0.3833	0.2182	11.0	0.7408	0.3379	0.2048	19	0.8060	0.3342	0.2013
4.0	0.6286	0.3696	0.2161	12.0	0.7516	0.3368	0.2042	20	0.8116	0.3344	0.2013
5.0	0.6485	0.3592	0.2139	13.0	0.7615	0.3361	0.2034	30	0.8528	0.3333	0.2007
6.0	0.6676	0.3519	0.2117	14.0	0.7705	0.3355	0.2028				
7.0	0.6852	0.3648	0.2100	15.0	0.7787	0.3351	0.2026				

Table 9 κ_i coefficient is for the first three modes

					κ_i						
k	κ_1	κ_2	κ_3	k	κ_1	κ_2	κ_3	k	κ_1	κ_2	κ_3
0.0		16.448	49.827	8.0	1.961	21.115	56.869	16	2.247	21.998	60.385
1.0	0.250	16.761	50.043	9.0	2.025	21.349	57.635	17	2.263	22.030	60.560
2.0	0.739	17.515	50.657	10.0	2.076	21.527	58.279	18	2.278	22.055	60.705
3.0	1.146	18.391	51.576	11.0	2.118	21.662	58.813	19	2.291	22.077	60.828
4.0	1.433	19.198	52.676	12.0	2.152	21.765	59.256	20	2.302	22.094	60.933
5.0	1.632	19.869	53.835	13.0	2.182	21.845	59.622	30	2.372	22.171	61.431
6.0	1.775	20.398	54.953	14.0	2.207	21.909	59.926				
7.0	1.881	20.737	55.973	15.0	2.228	21.959	60.176				

κ values are calculated and given in Table 9 for the first three modes.

As the structure gets higher, the more important the impact of the axial displacement of the columns becomes. In the method suggested in this study, the *K* shear rigidity coefficient is multiplied by a correction factor taken from the literature (Zalka 2000) in order to take these effects into consideration by approximation

$$K_s = s^2 * K \tag{43}$$

where the *s* coefficient is calculated using the following equation

$$s^2 = \frac{{f_g}^2}{{f_g}^2 + {f_s}^2} \tag{44}$$

where f_g and f_s indicates respectively, the frequencies constituted by only the axial displacements and only the shear displacements for the 1st mode. They are calculated using the following equation

$${f_g}^2 = \frac{0.313 * D * h}{H^4 * m} \tag{45}$$

$$f_s^{\,2} = \frac{K * h}{16 * H^2 * m} \tag{46}$$

D represents the global flexural rigidity representing the axial displacements. It is calculated using the following equation

$$D = E\sum_{i=1}^{q} A_{c,i} t_i^{\,2} \tag{47}$$

A_i shows the cross-sectional area of the i. column. t_i displays the distance of the column to the center of gravity.

3. The steps of this method

The steps of the suggested method are outlined below.

1) K, EI, and K_s values are calculated with the help of the Eqs. (2), (3), and (43).

2) k value is calculated using the equation no. (16)

3) S_i values are read from Table 1.

4) The periods of the first three modes are calculated using the Eq. (30).

5) Depending on the k parameter, eko_i (Table 3), ν_i (Table 5), η_i (Table 6), χ_i (Table 7), κ_i (Table 9) values are read from the relevant Tables for the first three modes.

6) The spectrum for the required earthquake record will be obtained.

7) With the help of Eq. (35), the top displacement is calculated for the first three modes.

8) With the help of Eq. (38), the maximum drift is calculated for the first three modes.

9) With the help of Eq. (39), the base shear forces are calculated for the first three modes.

10) With the help of Eq. (40), the overturning moments are calculated for the first three modes.

11) With the help of Eq. (42), the maximum bending moment is calculated for the first three modes.

12) The relevant displacements and internal forces of the system are calculated with the help of SRSS rule.

4. Numerical example

In this section, the response spectrum analysis of a 15-story building sample as illustrated in the Fig. 2 has been conducted in accordance with the Turkish Seismic Design Code using the suggested method in this study. The results are compared with the SAP2000 program in order to study the suitability. Shear wall is considered as equivalent frame element for the model in SAP2000 and the shear displacement is taken into consideration.

For the sample, the shear wall has been taken as 0.3 m/3 m, the columns as 0.3 m/0.6 m, and the beams as 0.25 m/0.50 m. The modulus of elasticity is $E=3*10^7$ kN/m^2.

The floor masses have been taken as 10 tons. Masses are acted on the floor levels in the analysis in SAP2000.

Acceleration and the displacement spectrum is based on the Turkish Seismic Design Code (2007). Accordingly, the acceleration and displacement spectrum is defined as follows

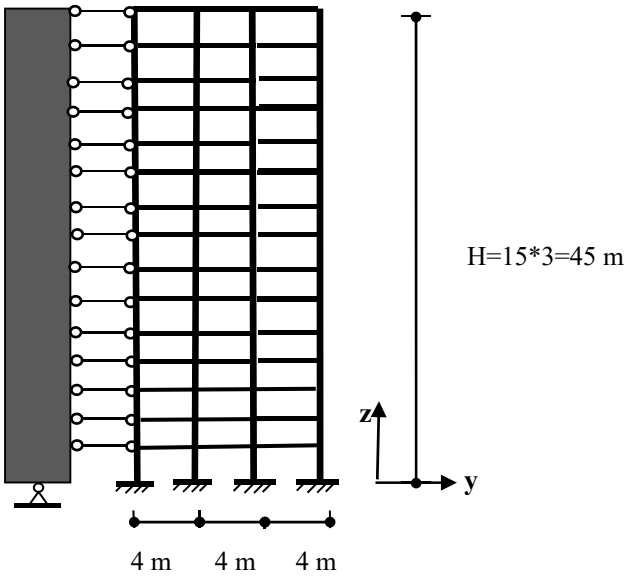

Fig. 2 15 storey wall frame

$$S_a(T) = \frac{A_0 * I * S(T)}{R_a} * g \tag{48}$$

$$S_d(T) = \frac{S_a(T)}{4\Pi^2} * T^2 \tag{49}$$

$$S(T) = 1 + 1.5 * \frac{T}{T_A} \qquad 0 \le T \le T_A \tag{50}$$

$$S(T) = 2.5 \qquad T_A < T \le T_B \tag{51}$$

$$S(T) = 2.5 * \left(\frac{T_B}{T}\right)^{0.8} \qquad T_B < T \tag{52}$$

$$R_a = 1.5 + (R - 1.5) * \frac{T}{T_A} \qquad 0 \le T \le T_A \tag{53}$$

$$R_a = R \qquad T_A < T \tag{54}$$

For this example, the values has been considered as, seismic zone is one and the site class Z4, importance factor is 1.0, seismic load reduction function has been taken as 8 in accordance with the Turkish Seismic Design Code. Thus

$$A_0 = 0.4 \qquad I = 1$$

$$For\ Z_4 \qquad T_A = 0.2 \qquad T_B = 0.9$$

$$R = 8$$

The acceleration spectrum used in the example is given in Fig. 3

The example has been analyzed by both taking into consideration the axial displacements and ignoring the axial displacements to show the contribution of the axial displacements.

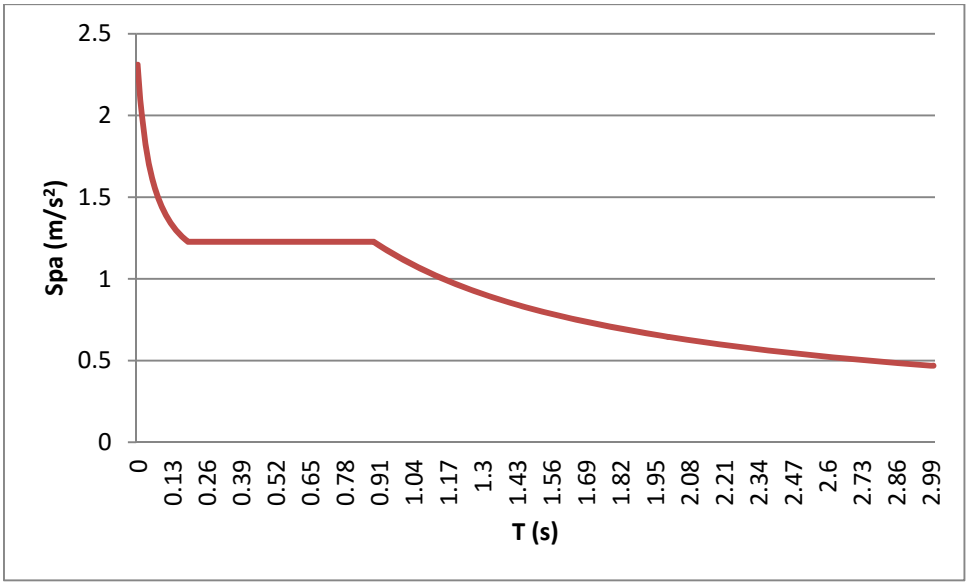

Fig. 3 The acceleration spectrum

Table 10 Parameters for the numerical example

	a	b
K	184353.9823 kN	157223.0014 kN
EI	20250000 kNm^2	20250000 kNm^2
D	-	432000000 kNm^2
k	4.29	3.965

Table 11 Necessary coefficients are required for the dynamic calculation of the case a (disregarding the axial displacements)

	1st mode	2nd mode	3rd mode
S_i	0.908	0.236	0.102
eko_i	0.80	0.106	0.036
v_i	1.36	0.59	0.39
η_j	1.885	1.804	1.909
χ_i	0.515	0.015	0.00178
κ_i	1.491	19.393	53.012

In the example given, the EI, K, D and k coefficients have been calculated first. They are shown in Table 10. The case a indicates the situation where the axial displacement is disregarded. Case b displays the situation where the axial displacement is taken into consideration.

The coefficients required for the dynamic analysis are given in Table 11 and Table 12 for the cases *a* and *b*.

Comparison of the periods calculated for the cases *a* and *b* to the SAP2000 are given in Table 13.

Table 12 Necessary coefficients are required for the dynamic calculation of the case *b* (taking the axial displacements into consideration)

	1st mode	2nd mode	3rd mode
S_i	0.973	0.247	0.105
eko_i	0.80	0.10	0.036
v_i	1.371	0.601	0.39
η_j	1.869	1.800	1.916
χ_i	0.516	0.0149	0.001586
κ_i	1.423	19.170	52.638

Table 13 Comparison of the periods

Mode	Case a	Case b	SAP2000
1	0.746 s	0.799 s	0.826 s
2	0.194 s	0.203 s	0.212 s
3	0.084 s	0.086 s	0.089 s

Table 14 Comparison between the top displacement and maximum drift ratio

	Case a	Case b	SAP2000
Peak displacement	0.024 m	0.027 m	0.0296 m
Maximum drift ratio	$7.263*10^{-4}$	$8.323*10^{-4}$	$7.667*10^{-4}$

Table 15 The comparison of the base shear force, overturning moment, and maximum bending moment values

	Case a	Case b	SAP2000
Base Shear Force	148.504 kN	148.88 kN	146.9 kN
Overturning Moment	4263.795 kNm	4285.894 kNm	4443.407 kNm
Max. Bending Moment	372.913 kNm	361.724 kNm	350.439 kNm

Considering the results provided in Table 13, it can be seen that the maximum error is -9.7% for the case where the axial displacements are not taken into consideration in the periods. While the maximum error is -4.25% for the case *b*, the axial displacements are taken into consideration.

The comparison of the top displacements and maximum drift ratio values are calculated for the cases *a* and *b* to the SAP2000 are given in Table 14.

Considering the results from Table 14, it can be understood that the maximum error is -18.92% for the case where the axial displacements are not taken into consideration for the top displacement compared to SAP2000. While the maximum error is -8.78% for the case **b** is where the axial displacements are taken into consideration.

As for the maximum drift ratio, this error -5.27% for the case *a*, and 8.56% for the case *b*.

The comparison of the base shear force, the overturning moment, and the maximum bending moment values as calculated for the cases *a* and *b* to the SAP2000 are given in Table 15.

As seen in Table 15, the maximum error is 1.1% for the case where the axial displacements are not taken into consideration for the base shear force compared to SAP2000. While the maximum

error is 1.35% for the case *b* where the axial displacements are taken into consideration.

As for the overturning moment, the error is -4.04% for the case *a* and -3.54% for the case *b*.

As for the maximum bending moment, the error for the case *a* is 6.41% and for the case *b* is 3.22%.

5. Conclusions

In this study, a method has been evaluated and suggested for the dynamic analysis of the frame-hinged shear wall structures. Structures have been analyzed in accordance with the continuous system calculation model and the parameters required for the dynamic analysis have been provided in each table of measurement. With the suggested method, the solution can be achieved practically and quickly by manual calculation. The compatibility of the method to the finite elements method has been studied on an example solved at the end of the study. With the results obtained, it has been observed that the method leads to certain results that are satisfactorily suitable for the finite elements method. In the analysis conducted, it has been considered that the axial displacements must be necessarily taken into consideration, particularly in high-rise buildings. It can be concluded that the suggested method can be used in understanding the dynamic behavior of structures with soft story irregularity using a few number of parameters and at the stage of preliminary design. The presented method can be applied to the analysis of the structures of variable cross section. In this case, the governing differential equation can be written with variable coefficients to get the solution.

References

Abidi, M. and Madhuri, M. (2012), "Review on shear wall for soft story high- rise buildings", *Int. J. Eng. Adv. Tech*., **1**(6).

Al-Aasam, H.S. and Mandal, P. (2013), "Simplified procedure to calculate by hand the natural periods of semirigid steel frames", *J. Struct. Eng*., ASCE, **139**(6), 1082-1087.

Baikov, V. and Sigalov, E. (1983), *Reinforced Concrete Structures*, Volume 2, Moscov: Mir Publisher, 390.

Balendra, T., Swaddiwudhipong, S. and Quek S.T. (1984), "Free vibration of asymmetric shear wall-frame buildings", *Earth. Eng. Struct. Dyn*., **12(**5), 629-650.

Basu, A., Nagpal, A. K,. and Kaul, S. (1984), "Charts for seismic design of frame-wall systems", *J. Struct. Eng. ASCE*, **110**(1), 31-46.

Belhadj, A.H. and Meftah, S.A. (2015), "Simplified finite element modelling of non-uniform tall building structures comprising wall and frame assemblies including P-Δ effects", *Earthq. Struct*., **8**(1), 253-273.

Bilyap, S. (1979), "An approximate solution for high- rise reinforced concrete panel buildings with combined diaphragms", *Int. J. Housing Sci*., **3**(6), 477-481.

Bozdogan, K.B. (2009), "An approximate method for static and dynamic analyses of symmetric wall-frame buildings", *Struct. Des. Tall Spec. Build*., **18**(3), 279-290.

Carpinteri, A., Lacidogna, G. and Cammarano, S. (2013), "Structural analysis of high- rise buildings under horizontal loads: A study on the Intesa Sanpaolo Tower in Turin", *Eng. Struct*., **56**, 1362-1371.

Colunga, A.T. (2010), "Review of the Soft Story High-Rise Buildings", *Open Civ. Eng. J*., **4**, 1-15.

Dym, C.L. and Williams, H.E. (2007), "Estimating fundamental frequencies of tall buildings", *J. Struct. Eng*., ASCE, **133**(10), 1479-1483.

Georgoussis, K.G. (2006), "A simple model for assessing and modal response quantities in symmetrical buildings", *Struct. Des. Tall Spec. Build*., **15(**2), 139-151.

Georgoussis, K.G. (2014), "Modified seismic analysis of multistory asymmetric elastic buildings and suggestions for minimizing the rotational response", *Earthq. Struct*., **7(**1), 39-55.
Heidebrecht, A.C. and Stafford Smith, B. (1973), "Approximate analysis of tall wall-frame buildings", *J. Struct. Eng*., ASCE, **99**(2), 199-221.
Hoenderkamp, D.C.J. (2001), "Elastic analysis of asymmetric tall buildings", *Struct. Des. Tall Build*., **10**(4), 245-261.
Hoenderkamp, D.C.J. (2002), "A simplified analysis of high-Rise structures with cores", *Struct. Des. Tall Build.*, **11**(2), 93-107.
Jahanshahi, M.R. and Rahgozar, R. (2012), "Free vibration analysis of combined sytem with variable cross section in tall buildings", *Struct. Eng. Mech*., **42(**4), 715-728.
Kazaz, I. and Gulkan, P. (2012), "An improved frame-shear wall model:continuum approach", *Struct. Des. Tall Spec. Build*., **21**(7), 524-542.
Kuang, J.S. and Ng, S.C. (2000), "Coupled lateral vibration of asymmetric shear wall structures", *Thin Wall. Struct*., **38**(2), 93-104.
Kuang, J.S. and Ng, C. (2009), "Lateral shear -St. Venant torsion coupled vibration of asymmetric -plan frame structures", *Struct. Des. Tall Spec. Build*., **18**(6), 647-656.
Kaviani, P., Rahgozar, R. and Saffari, H. (2008), "Approximate analysis of tall buildings using sandwich beam models with variable cross-section", *Struct. Des. Tall Spec. Build*., **17**(2), 401-418.
Laier, J.E. (2008), "An improved continuous medium technique for structural frame analysis", *Struct. Des. Tall Spec. Build*., **17**(1), 25-38.
Malekinejad, M. and Rahgozar, R. (2013), "An analytical approach to free vibration analysis of multi-outrigger-belt truss-reinforced tall buildings", *Struct. Des. Tall Spec. Build*., **22**(4), 382-398.
Mancini, E. and Savassi, W. (1999), "Tall buildings structures unified plane panels behavior", *Struct. Des. Tall Build*., **8**(2), 155-170.
Meftah, S.A. and Tounsi, A. (2008), "Vibration characteristics of tall buildings braced by shear walls and thin-walled open-section structures", *Struct. Des. Tall Spec. Build*., **17**(1), 203-216.
Miranda, E. (1999), "Approximate lateral drift demands in multi-story buildings subjected to earthquakes", *J. Struct. Eng*., ASCE, **125**(4), 417-425.
Miranda, E. and Reyes, J.C. (2002), "Approximate lateral drift demands in multi-story buildings with nonuniform stiffness", *J. Struct. Eng*., ASCE, **128**(7), 840-849.
Miranda, E. and Taghavi, S. (2005), "Approximate floor acceleration demands in multistorey buildings I formulation", *J. Struct. Eng*., ASCE, **131**(2), 203-211.
Ng, S.C. and Kuang, J.S. (2000), "Triply coupled vibration of asymmetric wall-frame structures", *J. Struct. Eng*., ASCE, **128**(7), 840-849.
Nollet, J.M. and Stafford Smith, B. (1993), "Behavior of curtailed wall-frame structures", *J. Struct. Eng*., ASCE, **119**(10), 2835-2853.
Pan, P., Wu, S. and Nie, X. (2015), "A distributed parameter model of a frame pin-supported wall structure", *Earthq. Eng. Struct. Dyn*, **44**(10), 1643-1659.
Potzta, G. and Kollar, L.P. (2003), "Analysis of building structures by replacement sandwich beams", *Int. J. Solid. Struct.*, **40**(3), 535-553.
Quanfeng, W., Lingyun, W. and Qiangsheng, L. (1999), "Seismic response of stepped frame-shear wall structures by using numerical method", *Comput. Method. Appl. Mech. Eng*., **173**(1), 31-39.
Rafezy, B., Zare, A. and Howson, W.P. (2007), "Coupled lateral -torsional frequencies of asymmetric, three dimensional frame structures", *Int. J. Solid. Struct*., **44(**1), 128-144.
Rafezy, B. and Howson, W.P. (2008), "Vibration analysis of doubly asymmetric, three dimensional structures comprising wall and frame assemblies with variable cross section", *J. Sound Vib.*, **318**(1-2), 247-266.
Reinoso, E. and Miranda, E. (2005), "Estimation of floor acceleration demands in high rise buildings during earthquakes", *Struct. Des. Tall Spec. Build*., **14**(2), 107-130.
Rodriguez, A.A. and Miranda, E. (2015), "Assesment of building behavior under near-fault pulse-like ground motions through simplified models", *Soil Dyn. Earthq. Eng*., **79**, 47-58.
Rosman, R. (1964), "Approximate analysis of shear walls subject to lateral loads", *Proc. Am. Concr. Inst*.,

61(6), 717-734.
Rosman, R. (1974), "Stability and dynamics of shear -wall frame structures", *Build. Sci.*, **9**, 55-63.
Rosman, R. (1981), "Buckling and vibrations of spatial building structures", *Eng. Struct*., **3**(4), 194-202.
Savassi, W. and Mancini, E. (2004), "One-dimensional finite element solution for tall building structures unified plane panels formulation", *Struct. Des. Tall Spec. Build*., **13**(4), 315-333.
Savassi, W. and Mancini, E. (2009), "One-dimensional finite element solution for non-uniform tall building structures and loading", *Struct. Des. Tall Spec. Build.*, **18**(4), 441-453.
Stafford Smith, B. and Crowe, E. (1986), "Estimating periods of vibration of tall buildings", *J. Struct. Eng*., ASCE, **112**(5), 1005-1019.
Swaddiwudhipong, S., Lee, L.S. and Zhou, Q. (2001), "Effect of the axial deformation on vibration of tall buildings", *Struct. Des. Tall Build.*, **10**(2), 79-91.
Taghavi, S. and Miranda, E. (2005), "Approximate floor acceleration demands in multistorey buildings II: applications", *J. Struct. Eng*., ASCE, **131**(2), 212-220.
Tarjan, G. and Kollar, P.L. (2004), "Approximate analysis of building structures with identical stories subjected to earthquakes", *Int. J. Solid. Struct*., **41**(5-6), 1411-1433.
Tekeli, H., Atimtay, E. and Turkmen, M. (2015), "An approximation method for design applications related to sway in RC framed buildings", *Int J.Civ. Eng*., **13**(3), 321-330.
Toutanji, H. (1997), "The effect of foundation flexibility on the interaction of walls and frames", *Eng. Struct*., **19**(12), 1036-1042.
Wang, S.K. (1997), "Stiffness, stability and fundemantal period of coupled shear walls of variable thickness", *Proc. Inst. Civ. Eng. Struct. Build.*, **122**(3), 334-338.
Wang, Y., Arnaouti, C. and Guo, S. (2000), "A Simple approximate formulation for the first two frequencies of asymmetric wall-frame multi-storey building structures", *J. Sound Vib*., **236**(1), 141-160.
Wdowicki, J. and Wdowicka, E. (2012), "Analysis of shear wall structures of variable cross section", *Struct. Des. Tall Spec. Build*., **21**(1), 1-15.
Yang, D., Pan, J. and Li, G. (2010), "Interstory drift ratio of building structures subjected to near-fault ground motions based on generalized drift spectral analysis", *Soil Dyn. Earthq. Eng*., **30**(11), 1182-1197.
Zalka, K.A. (2000), Global *Structural analysis of Buildings*, Taylor & Francis Group, Boca Raton, FL, USA.
Zalka, K.A. (2001), "A simplified method for calculation of natural frequencies of wall-frame buildings", *Eng. Struct*., **23(**12**)**, 1544-1555.
Zalka, K.A. (2009), "A simple method for the deflection analysis of tall-wall-frame building structures under horizontal load", *Struct. Des. Tall Spec. Build*., **18**(3), 291-311.
Zalka, K.A. (2013), *Structural analysis of regular multi-storey buildings*, Taylor & Francis Group, Boca Raton, FL, USA.
Zalka, K.A. (2014), "Maximum deflection of asymmetric wall-frame buildings under horizontal load", *Per. Poly. Civ. Eng*., **58**(4), 1-10.

CC